

Quantitative comparison of two independent lateral force calibration techniques for the atomic force microscope

Sarice S. Barkley, Zhao Deng, Richard S. Gates, Mark G. Reitsma, and Rachel J. Cannara

Citation: *Rev. Sci. Instrum.* **83**, 023707 (2012); doi: 10.1063/1.3685243

View online: <http://dx.doi.org/10.1063/1.3685243>

View Table of Contents: <http://rsi.aip.org/resource/1/RSINAK/v83/i2>

Published by the [American Institute of Physics](http://www.aip.org).

Related Articles

Constant tip-surface distance with atomic force microscopy via quality factor feedback

Rev. Sci. Instrum. **83**, 023706 (2012)

3D mechanical measurements with an atomic force microscope on 1D structures

Rev. Sci. Instrum. **83**, 023704 (2012)

Tapping-mode force spectroscopy using cantilevers with interferometric high-bandwidth force sensors

Appl. Phys. Lett. **100**, 053109 (2012)

Self-driving capacitive cantilevers for high-frequency atomic force microscopy

Appl. Phys. Lett. **100**, 053110 (2012)

Study of thermal and acoustic noise interferences in low stiffness atomic force microscope cantilevers and characterization of their dynamic properties

Rev. Sci. Instrum. **83**, 013704 (2012)

Additional information on *Rev. Sci. Instrum.*

Journal Homepage: <http://rsi.aip.org>

Journal Information: http://rsi.aip.org/about/about_the_journal

Top downloads: http://rsi.aip.org/features/most_downloaded

Information for Authors: <http://rsi.aip.org/authors>

ADVERTISEMENT



Quantitative comparison of two independent lateral force calibration techniques for the atomic force microscope

Sarice S. Barkley,^{1,a)} Zhao Deng,^{1,2,a)} Richard S. Gates,³ Mark G. Reitsma,^{3,b)} and Rachel J. Cannara^{1,c)}

¹Center for Nanoscale Science and Technology, National Institute of Standards and Technology, Gaithersburg, Maryland 20899, USA

²Maryland NanoCenter, University of Maryland, College Park, Maryland 20742, USA

³Material Measurement Laboratory, National Institute of Standards and Technology, Gaithersburg, Maryland 20899, USA

(Received 17 November 2011; accepted 28 January 2012; published online 15 February 2012)

Two independent lateral-force calibration methods for the atomic force microscope (AFM)—the hammerhead (HH) technique and the diamagnetic lateral force calibrator (D-LFC)—are systematically compared and found to agree to within 5 % or less, but with precision limited to about 15 %, using four different tee-shaped HH reference probes. The limitations of each method, both of which offer independent yet feasible paths toward traceable accuracy, are discussed and investigated. We find that stiff cantilevers may produce inconsistent D-LFC values through the application of excessively high normal loads. In addition, D-LFC results vary when the method is implemented using different modes of AFM feedback control, constant height and constant force modes, where the latter is more consistent with the HH method and closer to typical experimental conditions. Specifically, for the D-LFC apparatus used here, calibration in constant height mode introduced errors up to 14 %. In constant force mode using a relatively stiff cantilever, we observed an ≈ 4 % systematic error per μN of applied load for loads $\leq 1 \mu\text{N}$. The issue of excessive load typically emerges for cantilevers whose flexural spring constant is large compared with the normal spring constant of the D-LFC setup (such that relatively small cantilever flexural displacements produce relatively large loads). Overall, the HH method carries a larger uncertainty, which is dominated by uncertainty in measurement of the flexural spring constant of the HH cantilever as well as in the effective length dimension of the cantilever probe. The D-LFC method relies on fewer parameters and thus has fewer uncertainties associated with it. We thus show that it is the preferred method of the two, as long as care is taken to perform the calibration in constant force mode with low applied loads. [<http://dx.doi.org/10.1063/1.3685243>]

I. INTRODUCTION

The calibration of lateral forces in friction force microscopy has been an ongoing challenge for those who wish to quantify nanoscale friction and, ultimately, interfacial shear stress, using the atomic force microscope (AFM). Numerous methods have been developed for this purpose, as recently reviewed by Munz.¹ One key point of criticism expressed in this review article is that “a major means of assessing the resulting data is to cross-check if they are consistent with the values derived from several calibration routines.” In highlighting the need to develop accurate calibration standards, Munz is referring to an earlier work by Cain *et al.*,² in which a comparison among the optical geometry method,³ the lateral compliance method,⁴ and the wedge method⁵ was performed. The practical advantages and disadvantages of implementing each technique were reviewed. The optical geometry method determines the detector response, but this is based on modeling the optical path from the cantilever to the detector; the lateral compliance method proves a simple solution for spherical

probes for which the effect of contact and probe stiffness may be neglected, but only under certain conditions. A significant advantage of the wedge method is that it derives the lateral force calibration factor without the need for the torsional spring constant of the cantilever or the lateral deflection sensitivity of the photodiode (normal sensitivities are typically required in the majority of calibration methods); however, it requires that multiple friction measurements be made, which can cause tip damage. Otherwise, the ability to eliminate cross-talk must be sacrificed.^{6,7} The difficulty in comparing these three methods is that underlying assumptions in each method lead to potentially large inaccuracies, and the true value for the force calibration factor is not well established. In light of current uncertainty over which method is “best,” it is preferable to evaluate lateral force calibration methods first and foremost based on their accuracy and precision, as opposed to relative ease of use. In this article, two methods are investigated, the hammerhead (HH) technique^{8,9} and the diamagnetic lateral force calibrator (D-LFC),¹⁰ which both offer independent, yet feasible paths toward traceable accuracy. In addition to relatively straightforward implementation, principle loads for respective techniques are applied orthogonally and no critical variables are shared, thus facilitating an explicit and robust comparison of lateral force calibration methods.

a) Sarice S. Barkley and Zhao Deng contributed equally to this work.

b) Electronic mail: mark@asylumresearch.com.

c) Author to whom correspondence should be addressed. Electronic mail: rachel.cannara@nist.gov.

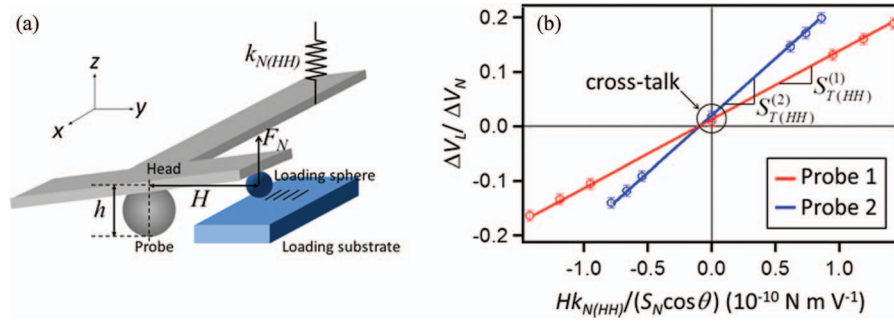


FIG. 1. (Color online) (a) Schematic illustration of the HH calibration technique. (b) $\Delta V_L/\Delta V_N$ for Probes 1 and 2 plotted as a function of $Hk_{N(HH)}/(S_N \cos \theta)$, where the pivot position, H , is varied, thereby obtaining the torque sensitivity (or slope), $S_{T(HH)}$, for each probe.

In lateral force microscopy, friction at the probe-surface interface occurs as the probe slides relative to the surface in a direction orthogonal to the long axis of the cantilever (i.e., the x -axis). During sliding (in the y -direction), the friction force, F_f , couples to the probe moment arm, causing the cantilever to twist. The response of the instrument detector to cantilever twist is ΔV_L . The lateral force sensitivity of the optical lever system, S_L , is used to quantify the friction force at the probe-surface interface according to $F_f = \Delta V_L/S_L$. In this work, S_L is used as a basis for quantitative comparison between the HH and D-LFC calibration methods.

The HH method utilizes a tee-shaped cantilever to quantify the lateral (or torsional) signal sensitivity by analyzing the ratio between flexural and torsional signals in response to calculable force and torque applied to the cantilever. The principle of this calibration method is illustrated in Fig. 1(a) and described as follows: A normal load, F_N , is imposed at a distance, H , along the arm of the tee by pressing it against a loading sphere that is glued to the edge of a stiff surface on which fiducial marks are used to calculate the pivot position. The applied torque produces both flexural and torsional responses in the cantilever and is given by

$$\frac{T_{HH}}{\cos \theta} = F_N \times H = \frac{\Delta V_N k_{N(HH)}}{S_N \cos^2 \theta} H, \quad (1)$$

where ΔV_N is the change in normal signal when pressing against the loading sphere, S_N is the normal signal sensitivity of the optical lever system, $k_{N(HH)}$ is the flexural spring constant of the cantilever, and θ is the angle of the cantilever with respect to the nominal x - y sample plane (required here to account for both the force normal to the sample surface and the true deflection of the free end of the cantilever).¹¹ The change in torsional signal, ΔV_L , in response to torque, T_{HH} , is given by $\Delta V_L = S_{T(HH)} \times T_{HH}$, where $S_{T(HH)}$ is the torque sensitivity of the optical lever system. Combining this relation with Eq. (1) yields

$$S_{T(HH)} = \left(\frac{\Delta V_L}{\Delta V_N} \right) / \left(\frac{H k_{N(HH)}}{S_N \cos \theta} \right). \quad (2)$$

Therefore, if $k_{N(HH)}$ and S_N are known, the ratio $\Delta V_L/\Delta V_N$, acquired from vertical force-displacement curves, may be plotted as a function of the denominator in Eq. (2), where H is varied by stepping along the fiducial marks in the loading surface. $S_{T(HH)}$ is then obtained from the slope of the linear fit, as in Fig. 1(b), which shows HH calibration data for two dif-

ferent cantilever probes. Illustrated in Fig. 1(a), the effective probe length, h , extends from the shear center of the cantilever (about which twisting occurs) to the apex of the probe (where it contacts the surface). For a probe length, h , the lateral force sensitivity of the optical lever system can be defined as

$$S_{L(HH)} \equiv h S_{T(HH)} = h \left(\frac{\Delta V_L}{\Delta V_N} \right) / \left(\frac{H k_{N(HH)}}{S_N \cos \theta} \right). \quad (3)$$

For the specific hammerhead cantilevers used in this work, flexural bending of the HH cantilever wings during calibration is expected to produce errors of $< 3\%$ for the accurate measurement of lateral friction forces (this error could be reduced or practically eliminated by using HH cantilevers with stiffer wings), according to finite element analysis conducted by Reitsma *et al.*⁹ Nevertheless, this prediction does not address actual experimental uncertainty, which Reitsma *et al.* found to be $< 1\%$ in their determination of $S_{T(HH)}$, owing to a small uncertainty in their $k_{N(HH)}$ measurement. However, for the measurement of lateral (friction) forces, S_L is required, and from Eq. (3) an additional significant source of error in the HH method arises from measurement uncertainty in the probe dimension, $h = d + (t/2)$, where d is the diameter of the spherical colloidal probe (or length of the integrated tip) and t is the cantilever thickness at the probe position.

The D-LFC method developed by Li *et al.*¹⁰ does not require foreknowledge of any property of the cantilever and may be applied to most AFM probes. As shown in Fig. 2(a), the D-LFC method employs a pre-calibrated spring (a diamagnetically levitated graphite substrate) with (lateral) spring constant, $k_{L(D-LFC)}$, to apply a torque to the cantilever through static friction at the probe tip. The spring is composed of a square piece of pyrolytic graphite and four permanent magnets with neighboring opposite poles. The lateral force, F_L , on the cantilever is given by

$$F_L = k_{L(D-LFC)} \Delta y, \quad (4)$$

where Δy is the lateral displacement of the magnets relative to the cantilever base, and $k_{L(D-LFC)}$ is calculated by measuring the mass, m , and vibrational frequency, f , of the levitated graphite substrate using the equation $k_{L(D-LFC)} = m(2\pi f)^2$. Hence, the lateral force sensitivity can be expressed as

$$S_{L(D-LFC)} \equiv \frac{\Delta V_L}{F_L} = \frac{\Delta V_L}{(k_{L(D-LFC)} \Delta y)}, \quad (5)$$

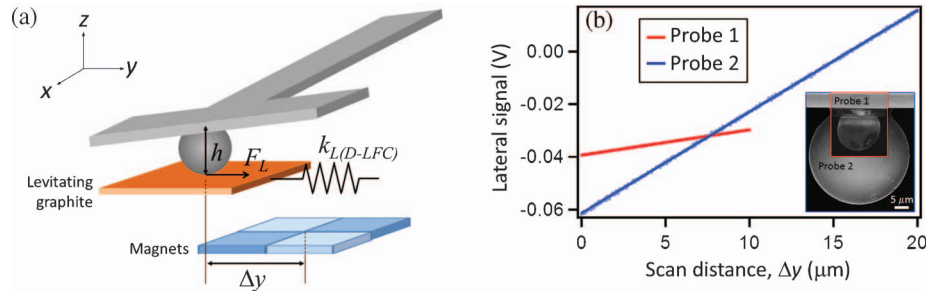


FIG. 2. (Color online) (a) Schematic illustration of the D-LFC setup. (b) D-LFC data and linear fits for Probes 1 and 2. Inset: SEM images of Probes 1 and 2.

where ΔV_L is the change in lateral signal with stage displacement, Δy , which is assumed to be equal to the displacement of the graphite piece. This assumption holds for the typical case when the cantilever torsional spring constant is much greater than $k_{L(D-LFC)}$, as satisfied by the cantilevers used in this article. Note that we have differentiated between F_L and F_f , because F_L is a static friction force in the D-LFC measurement, and F_f corresponds to the sliding (dynamic) friction forces to be calibrated.

Comparing the two methods, we note that not a single parameter in Eqs. (3) and (5) is shared, and each approach obtains signal sensitivities from orthogonally applied forces. The HH method determines S_L based on the ratio of lateral and normal signals obtained from vertical force-displacement curves; whereas, in the D-LFC, S_L is extracted from the lateral displacement of the graphite substrate. Accordingly, the spring constants and lever arms of each method are orthogonal. Thus, this serves as a highly controlled comparison which, if consistent, validates both methods unambiguously.

II. EXPERIMENTAL

In this study, we systematically compared the S_L value obtained from the HH method and from the D-LFC using the same HH cantilever, with a total of four different cantilevers, as summarized in Table I below. All measurements were performed on a Cypher AFM (Asylum Research, Inc., Santa Barbara, CA),¹² which has a built-in cantilever an-

gle $\theta = 11^\circ$. Each HH cantilever used was $50 \mu\text{m}$ wide between the head and fixed-end with a head that extended $150 \mu\text{m}$ in width (y -dimension, Fig. 1(a)). In Table I, the length and width dimensions of each cantilever are listed along with probe diameters—all determined using scanning electron microscopy (SEM); SEM images of Probes 1 and 2 are shown in the inset of Fig. 2(b). Cantilever thickness was measured using a white light interferometric microscope. Flexural spring constants were calculated using the thermal spectrum method.^{13,14} To determine the lateral spring constant of the balance in the D-LFC method, the mass of the $(6 \times 6 \times 1) \text{ mm}^3$ levitated graphite piece was determined and its in-plane vibrational frequency along the sliding direction (parallel to the short axis of the cantilever) was tracked using a high-speed camera with a frame rate of 420 s^{-1} and analyzed using a software routine. The dimensions of the magnets used in this study were $(0.635 \times 0.635 \times 0.318) \text{ mm}^3$ (Part # B442, K & J Magnetics, Inc.).¹²

Figures 1(b) and 2(b) show representative data for both methods from which S_L was calculated, where data were collected for each method without disturbing the optical lever system between methods. In Fig. 1(b), each $\Delta V_L/\Delta V_N$ value from the HH calibration was obtained by averaging five sets of normal and lateral force distance curves taken at the corresponding lever arm.⁹ The points centered on $H = 0$ came from force distance curves taken on a flat silicon surface; the small offset from the origin is a result of system cross-talk. Figure 2(b) shows the lateral voltage as a function of lateral

TABLE I. Measured and calculated parameters for the four tee-shaped cantilever probes.

	Probe 1	Probe 2	Probe 3	Probe 4
Length, l (μm)	300 ± 1	300 ± 1	500 ± 1	500 ± 1
Cantilever width (μm)	50 ± 1	50 ± 1	50 ± 1	50 ± 1
Head width (μm)	150 ± 1	150 ± 1	150 ± 1	150 ± 1
Thickness, t (μm)	5.8 ± 0.1	5.8 ± 0.1	5.8 ± 0.1	2.8 ± 0.1
Probe diameter, d (μm)	15 ± 1	40 ± 2	40 ± 2	40 ± 2
Cantilever flexural spring constant $k_{N(\text{HH})}$ (N m^{-1})	16.3 ± 0.8	13.3 ± 0.7	3.2 ± 0.2	0.37 ± 0.02
Cantilever lateral spring constant $k_{L(\text{HH})}$ (N m^{-1})	1575.2 ± 297.2	216.2 ± 25.6	91.7 ± 14.3	9.32 ± 1.35
Total signal (V)	3.73 ± 0.02	6.32 ± 0.03	4.43 ± 0.03	4.98 ± 0.04
$\Delta\zeta$ ($\text{nN}^{-1} \text{ m}^{-1}$) ^a	0.339 ± 0.030	0.336 ± 0.022	0.577 ± 0.041	4.93 ± 0.32
$S_{L(\text{HH})}$ ($\times 10^5 \text{ V N}^{-1}$) ^b	0.221 ± 0.024 (11 %)	0.876 ± 0.098 (11 %)	1.044 ± 0.081 (7.8 %)	10.02 ± 1.18 (12 %)
$S_{L(\text{D-LFC})}$ ($\times 10^5 \text{ V N}^{-1}$) ^c	0.228 ± 0.017 (7.5 %)	0.912 ± 0.061 (6.7 %)	1.096 ± 0.076 (6.9 %)	10.19 ± 0.60 (5.9 %)
Discrepancy (%)	3.1 ± 13.2	4.0 ± 13.0	4.9 ± 10.4	1.7 ± 11.8

^a $\Delta\zeta$ is the change in lateral signal normalized to (divided by) the total signal and the applied torque ($k_{L(\text{D-LFC})} \times \Delta x$) in the D-LFC method.

^bUncertainty values carry a nominal statistical uncertainty of 5% for the cantilever flexural spring constant, $k_{N(\text{HH})}$.

^cUncertainty values carry a nominal statistical uncertainty of 5% for the lateral spring constant, $k_{L(\text{D-LFC})}$, of the levitating graphite piece.

displacement for the D-LFC calibration of Probes 1 and 2. Individual data points were averaged from 64 scan lines and fit to a line. In both Figures 1(b) and 2(b), error bars are given by one standard deviation. The uncertainties listed in Table I are calculated from the usual Taylor series expansion approach for propagating error and include one standard deviation.¹⁵

III. RESULTS AND DISCUSSION

A. Lateral force sensitivity

Table I shows results for all four probes, along with discrepancies between the two calibration methods, calculated from $2|\bar{S}_{L(HH)} - \bar{S}_{L(D-LFC)}|/(\bar{S}_{L(HH)} + \bar{S}_{L(D-LFC)})$, which ranged from 1.7% to 4.9%. The excellent agreement between the methods was found despite a 6%–12% associated uncertainty in each individual S_L , based on error propagation from Eqs. (3) and (5). Here, since traceable accuracy of $k_{N(HH)}$ for these cantilevers has not yet been established, we have applied a nominal value of 5% for the statistical uncertainty in determining $k_{N(HH)}$ by the thermal noise method as determined for colloidal (spherical) probes by Chung *et al.*¹⁴ While the statistical uncertainty in the present experiment was 0.5%, we assumed this to be incorporated into an expected nominal overall statistical uncertainty of 5%, which we then propagated along with the measurement precision and the relative uncertainties for the other factors contributing to $S_{L(HH)}$. The close agreement between the two calibration methods is surprising, considering the potential measurement errors associated with $k_{N(HH)}$ and $k_{L(D-LFC)}$, which are the major sources of uncertainty for each method. To calculate $k_{N(HH)}$, the thermal noise model treats the AFM cantilever as a simple harmonic oscillator and dynamic cantilever displacement is quantified using quasi-static force curves; further, to accurately derive $k_{L(D-LFC)}$, only translational motion of the graphite substrate must be excited—a challenging task, where small errors arise due to minor amounts of rotational motion. Taking into account all uncertainties, we find that the total discrepancy between these two lateral calibration methods is about 15% from the study conducted here (see Table I).

We further compared Probes 1 and 2, which are the same cantilever-type but have different sphere diameters, to check the consistency of the D-LFC method. Figure 2(b) shows the lateral calibration of both probes using the D-LFC method. When calibrating Probe 1, a total lateral displacement, Δy , of 10 μm was chosen in order to avoid sliding which can arise due to the small contact area between the small sphere and the surface. For Probe 2, however, a larger Δy of 20 μm could be used. For the same cantilever-type but different probe sizes (e.g., for Probes 1 and 2), normalization of ΔV_L to the total torque ($k_{L(D-LFC)} \times \Delta y$) and to the total signal should produce identical values. To demonstrate this, we calculated the normalized values of ΔV_L ($\Delta\zeta$ in Table I) and found that they agree to within less than 1% for Probes 1 and 2, which is indicative of good precision in the D-LFC calibration.

B. Effect of applied load on D-LFC calibration

In the D-LFC method, probes with high flexural stiffness, such as Probes 1 and 2, are capable of pressing the

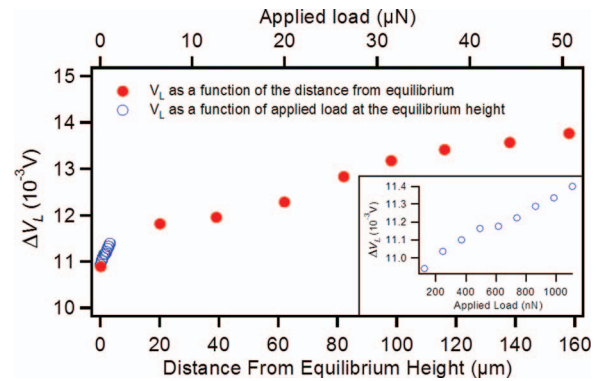


FIG. 3. (Color online) ΔV_L for Probe 2 for the same lateral displacement ($\Delta y = 20 \mu\text{m}$) but different applied loads (open blue circles) and more extreme vertical displacements (closed red circles) of the graphite substrate from its equilibrium levitation height. Upper abscissa shows corresponding applied load. Inset: Expanded region near zero vertical displacement but varying load in constant force mode.

levitating graphite substrate downward, causing the graphite to deviate significantly from the equilibrium height at which $k_{L(D-LFC)}$ is obtained. We identified relatively stiff cantilevers and investigated the effect of this deviation on S_L . Using the reference cantilever method^{16,17} and correcting the vertical force vector for the mounting angle of the cantilever,¹¹ with Probe 2 as the “reference” cantilever, we estimated the normal stiffness, $k_{N(D-LFC)}$, of the D-LFC setup from vertical force-displacement curves taken on the levitating graphite piece (versus vertical force-displacement curves taken on a relatively rigid silicon substrate) and found that $k_{N(D-LFC)} = 0.32 \pm 0.03 \text{ N/m}$. Thus, Probes 1 and 2 are very stiff compared with the D-LFC setup (see Table I), and we found that these probes were particularly prone to displacing the levitating graphite piece, but not Probes 3 and 4. In Fig. 3, Probe 2 was used to vary the applied load and to displace the substrate in the vertical direction by a known amount, where zero load corresponds to the equilibrium height. First, a series of ΔV_L values were taken for the same lateral displacement, Δy , by varying the normal signal setpoint (i.e., applied load) while maintaining the graphite close to the equilibrium height. Based on these data, an $\approx 4\%$ increase in ΔV_L was observed for an approximately ten-fold increase in load, from $\approx 100 \text{ nN}$ to $1 \mu\text{N}$.

Going out of the vertical displacement range of the normal setpoint control, we then manually pressed the cantilever down using the coarse motion provided by the motorized probe holder and observed a dramatic increase in ΔV_L (for a given Δy) as a function of the distance of the substrate from its equilibrium height (Fig. 3). Specifically, ΔV_L increased by more than 25% over the range of heights (loads) tested. Hence, it can be concluded that, when using the D-LFC method to calibrate probes with high flexural stiffness, one must be very careful to avoid the application of excessive load that will cause deviation of the graphite from its equilibrium height. Otherwise, the pre-calibrated $k_{L(D-LFC)}$ will no longer be applicable, leading to significant calibration error. We note that when calibrating probes with softer cantilevers, such as Probes 3 and 4, such deviation was negligible. For the D-LFC apparatus used in this work, we found that

systematic errors due to variations in ΔV_L as a function applied load ranged from $\approx 4.4\%$ per μN at low loads ($<1\ \mu\text{N}$), diminishing to an average of $\approx 0.7\%$ per μN for loads greater than $1\ \mu\text{N}$ (and up to $\approx 40\ \mu\text{N}$ studied here). This error may vary with the strength and shape of the magnetic field, and potentially the mass of the levitating graphite piece, and should thus be determined for the specific apparatus and calibration setup used.

C. D-LFC constant height vs. constant force mode

We compared S_L values obtained from the D-LFC with the AFM instrument set to constant height mode versus constant force mode. In the D-LFC method, operating in constant height mode consists of turning off the force feedback and holding the vertical distance between the magnets and the base of the cantilever fixed. Thus, the magnets (or cantilever base, depending on the AFM design) are actuated only along the lateral (y) direction, and the sphere-graphite interface is free to move, e.g., along the vertical (z) direction. In constant force mode, force feedback is kept on, the magnets move along both the lateral and vertical directions in order to maintain a constant flexural angle of deflection of the cantilever, and no vertical motion of the interface should occur. Due to the extra effort required to stabilize the feedback loop when working with this levitated system, it is tempting to avoid force feedback and use constant height mode with the D-LFC. We consistently find, however, that a higher ΔV_L per Δy is obtained in constant height mode. Depending on the type of probe used, this discrepancy in ΔV_L can be significant, up to 14% for other (non-HH) probes not reported here. Using HH Probe 4, we measured the change in ΔV_L as a function of lateral displacement for constant force and constant height modes. Relative to constant force mode, a 2.5% increase in ΔV_L was observed using a constant height mode with the piezo maintained at the mean voltage used to acquire constant force data. Results from the constant force mode consistently lead to greater agreement with the HH method. We believe the higher ΔV_L value obtained with the constant height mode represents an intrinsic behavior of the D-LFC calibrator, arising from the spatial distribution of the magnetic field and normal-lateral coupling in the optical lever system, since force and torque applied to the cantilever during lateral motion are not well controlled when the feedback gains are low or off.

D. HH vs. D-LFC discussion

Our results show that the discrepancy in S_L between the HH and D-LFC methods is fairly small ($<5\%$). However, one must be careful, as the uncertainty associated with each S_L value is greater than this value (Table I). The small mean discrepancy demonstrates an overall consistency between the two methods, and it indicates good control over experimental conditions, but the total uncertainty in the discrepancy value is greater than 10% . Tracking the sources of error in the HH method based on Eq. (3) yields uncertainties associated with the calculation of $\Delta V_L/\Delta V_N$, the effective probe lever arm (h), the lateral lever arm (H), the normal signal sensitivity (S_N), and the flexural spring constant of the cantilever

($k_{N(\text{HH})}$). Among these parameters, the uncertainties associated with $\Delta V_L/\Delta V_N$ and S_N are mainly statistical uncertainties, which we determined from the standard deviation of multiple measurements; the determination of h has uncertainty associated with the method by which it was measured, SEM in this case; uncertainties in H arise from misalignment of the edge of the HH with the fiducial marks on the substrate as viewed by the optical microscope built into the AFM. Based on user positioning repeatability in addition to the diffraction-limited resolution of the AFM view module used, we estimate an error of $\pm 2\ \mu\text{m}$ in measurement of H . We also note the error contributed by H is minimized by plotting $\Delta V_L/\Delta V_N$ as a function of H . In the HH method, the largest sources of error are in the determination of the probe length dimension, h , and in the flexural spring constant of the cantilever, $k_{N(\text{HH})}$. In our case, $k_{N(\text{HH})}$ was measured using the thermal spectrum method, based on modeling the AFM cantilever as a simple harmonic oscillator. As discussed, this approximation typically results in a conservative statistical uncertainty of $\approx 5\%$ for the flexural spring constant.¹⁴

In contrast, from Eq. (5), only three sources of error contribute to the D-LFC method. The uncertainty associated with ΔV_L is again primarily due to statistical variations, as determined from the standard deviation of multiple measurements. The error in Δy can be neglected, as positioning uncertainty is less than $0.1\ \text{nm}$. This leaves $k_{L(\text{D-LFC})}$ as the main error source. The equation used to calculate $k_{L(\text{D-LFC})}$, $k_{L(\text{D-LFC})} = m(2\pi f)^2$, is an approximation and was reported to result in an error of less than one part in 10^4 ;¹⁰ therefore, the main uncertainty in the D-LFC method arises from the mass and oscillation frequency of the levitated substrate. We determined the mass using a high-precision balance and obtained the value $m = (18.5 \pm 0.2)\ \text{mg}$, where the uncertainty is one standard deviation. For the oscillation frequency, we obtained a value $f = (7.7 \pm 0.2)\ \text{Hz}$ after repeated measurements with the coupling from rotational motion minimized. All of these individual errors were propagated based on Eqs. (3) and (5) to obtain the final uncertainty values listed in Table I, from which one can see that the D-LFC method exhibits significantly less uncertainty compared with the HH method. The lateral spring constant of the levitating graphite piece was measured to be $k_{L(\text{D-LFC})} = (0.043 \pm 0.002)\ \text{N m}^{-1}$. This value is far less than the lateral spring constants ($k_{L(\text{HH})}$) of the cantilevers, obtained here via the HH method⁹ (Table I). The relation $k_{L(\text{D-LFC})} \ll k_{L(\text{HH})}$ is a prerequisite for using the D-LFC method.

Cross talk in AFM optical lever systems is known to be problematic for many lateral force calibration methods. Generally two forms of system cross talk can occur: Optical cross talk is caused by a misalignment of the cantilever's reflective surface with the sector axis of the quad-cell photodetector, which results in a convolution of normal and lateral signals during force measurement. Mechanical cross talk occurs when torque is present in the cantilever even when a torque has not been deliberately applied. This is typically caused by a probe that is misaligned with respect to the shear center of the cantilever. In the HH method, optical cross talk has been shown to have a negligible effect on the determination of torque sensitivity, $S_{T(\text{HH})}$, despite the misalignment being

obvious from calibration data, as shown in Fig. 1(a).⁹ Mechanical cross talk can also be detected in the HH method from $S_{T(HH)}$ data¹⁸ and can be problematic for the interpretation of force and torque in the method. Mechanical cross talk is unlikely to affect the measurement of lateral force in the D-LFC method. On the other hand, optical cross talk will likely impact the D-LFC method with respect to the control of applied load. In fact, optical cross talk will impact all load-controlled (constant force) lateral force measurements because of the convolution of normal and lateral detector signals: A change in lateral output, as the cantilever twists, will produce a change in normal output, which in turn will cause the active feedback loop to adjust the apparent load dynamically from one twisting direction to the other. The implication is that the actual load will be changed rather than maintained, and this change will be a function of the direction and magnitude of cantilever twist.⁹ We note that this effect should be small in most cases, but not necessarily negligible.

In general, the D-LFC may be more useful for its applicability to any cantilever type. A different form of the HH method has been demonstrated for use with commercially available rectangular cantilevers, but it requires an AFM instrument with closed-loop positioning.¹⁸ A disadvantage for both HH and D-LFC methods, as described above, is the need to contact the probe to a calibration surface, thereby risking contamination or wear; however, neither approach requires sliding. Contact between the probe and calibration surface can be avoided in the HH method if alternative methods are used to obtain signal sensitivities at $H = 0$.¹⁴ A non-contact approach is also crucial if hysteresis arises in the normal force-displacement curves (at $H = 0$).^{19,20} Probe-surface contact could also be avoided using the HH method by determining the $H = 0$ value from linear interpolation of the $H \neq 0$ data (Fig. 1(b)); however, care should be taken to ensure that the system is free of mechanical cross talk.¹⁸

Using the HH method as a basis for optimizing the D-LFC method, we found that a relatively stiff cantilever is capable of pushing the levitating substrate away from its equilibrium height, leading to significant systematic error in the measurement. In addition, comparison of constant height and constant force modes for the D-LFC method reveals a slight discrepancy in calibration results, where the latter is more consistent with the HH method and closer to typical measurement conditions. Thus, when calibrating lateral forces using the D-LFC method, one should be aware of the discrepancy between the constant height and constant force modes.

IV. CONCLUSION

In summary, we have systematically compared two lateral force calibration methods: the HH method and the D-LFC method. Performed on each of four different cantilever-probes, we believe that this was a well-controlled assessment, comparing two methods that did not share any critical parameters and in which cantilever torque was induced via

respectively orthogonal loads. Furthermore, both methods offer a potential path toward accurate measurements, which could be implemented as part of future standardization work. Calibration results for four HH probes produced a strong agreement between the two methods, with a discrepancy of $< 5\%$ in the lateral calibration sensitivity, S_L , obtained from the comparison experiments reported here. However, one must keep in mind that the measurement uncertainty (up to 12%) associated with these S_L values is higher than the mean discrepancy. Nonetheless, these results confirm overall consistency between the two methods. If contact between the probe and the calibration surface must be avoided, the HH method is advantageous, despite carrying greater measurement uncertainty. The D-LFC method relies on fewer parameters and thus has fewer uncertainties associated with it. It is thus preferred overall, if care is taken to perform the calibration in constant force mode with low applied loads.

ACKNOWLEDGMENTS

We thank Erin Flater and Gordon Shaw for helpful discussions regarding this work. S.S.B. is grateful to the 2011 National Institute of Standards and Technology (NIST) Summer Undergraduate Research Fellowship program for financial support.

¹M. Munz, *J. Phys. D: Appl. Phys.* **43**, 063001 (2010).

²R. G. Cain, M. G. Reitsma, S. Biggs, and N. W. Page, *Rev. Sci. Instrum.* **72**, 3304 (2001).

³E. Liu, B. Blanpain, and J. P. Celis, *Wear* **192**, 141 (1996).

⁴R. G. Cain, S. Biggs, and N. W. Page, *J. Colloid Interface Sci.* **227**, 55 (2000).

⁵D. F. Ogletree, R. W. Carpick, and M. Salmeron, *Rev. Sci. Instrum.* **67**, 3298 (1996).

⁶M. Varenberg, I. Etsion, and G. Halperin, *Rev. Sci. Instrum.* **74**, 3569 (2003).

⁷M. Varenberg, I. Etsion, and G. Halperin, *Rev. Sci. Instrum.* **74**, 3362 (2003).

⁸M. G. Reitsma, *Rev. Sci. Instrum.* **78**, 106102 (2007).

⁹M. G. Reitsma, R. S. Gates, L. H. Friedman, and R. F. Cook, *Rev. Sci. Instrum.* **82**, 093706 (2011).

¹⁰Q. Li, K. S. Kim, and A. Rydberg, *Rev. Sci. Instrum.* **77**, 065105 (2006).

¹¹S. A. Edwards, W. A. Ducker, and J. E. Sader, *J. Appl. Phys.* **103**, 064513 (2008).

¹²The full description of the procedures used in this article requires the identification of certain commercial products and their suppliers. The inclusion of such information should in no way be construed as indicating that such products or suppliers are endorsed by NIST or are recommended by NIST or that they are necessarily the best materials, instruments, software or suppliers for the purposes described.

¹³D. A. Walters, J. P. Cleveland, N. H. Thomson, P. K. Hansma, M. A. Wendman, G. Gurley, and V. Elings, *Rev. Sci. Instrum.* **67**, 3583 (1996).

¹⁴K. H. Chung, G. A. Shaw, and J. R. Pratt, *Rev. Sci. Instrum.* **80**, 065107 (2009).

¹⁵B. N. Taylor and C. E. Kuyatt, NIST Technical Note No. 1297 (1994).

¹⁶A. Torii, M. Sasaki, K. Hane, and S. Okuma, *Meas. Sci. Technol.* **7**, 179 (1996).

¹⁷C. T. Gibson, G. S. Watson, and S. Myhra, *Nanotechnology* **7**, 259 (1996).

¹⁸K. H. Chung and M. G. Reitsma, *Rev. Sci. Instrum.* **81**, 026104 (2010).

¹⁹J. R. Pratt, G. A. Shaw, L. Kumanchik, and N. A. Burnham, *J. Appl. Phys.* **107**, 044305 (2010).

²⁰No statistically significant approach-retract hysteresis was observed in this work.